

Progress of the Ubaye hypertelescope project

D. Mourard¹ · A. Labeyrie^{2,3} · T. Lepage^{4,5} ·
P. D. Nunez^{1,6} · B. Tregon⁷ · Z. Xie^{1,8}

Received: 15 January 2018 / Accepted: 16 April 2018 / Published online: 28 June 2018
© Springer Nature B.V. 2018

Abstract In this paper we present the principle of the prototype hypertelescope built in the valley of Ubaye in the Southern Alps. We detail the most representative results obtained during the last campaign of tests in August and September 2017. We conclude the paper by summarizing some of the other activities that we are developing toward the future implementation of an ambitious astronomical hypertelescope.

Keywords High angular resolution · Hypertelescope

This article is part of the Topical Collection on *Future of Optical-infrared Interferometry in Europe*

✉ D. Mourard
denis.mourard@oca.eu

¹ Université Côte d'Azur, OCA, CNRS, Lagrange, Parc Valrose, Bât. Fizeau, 06108 Nice cedex 02, France

² Collège de France, Paris, France

³ Université Côte d'Azur, OCA, CNRS, Lagrange, 2130 Route de l'Observatoire, 06460 Caussols, France

⁴ Institut d'Optique Graduate School, 18 rue Benoit Luras, 42000 Saint-Etienne, France

⁵ Université de Lyon, CNRS, Laboratoire Hubert Curien (UMR 5516), 18 Rue Benoit Luras, F-42000, Saint-Etienne, France

⁶ Present address: MDA Systems, 13800 Commerce Pkwy, Richmond, BC V6V 2J3, Canada

⁷ Université de Bordeaux, CNRS, LOMA, 351 cours de la libération, 33405 Talence Cedex, France

⁸ Present address: Key Laboratory of Optical Engineering, Institute of Optics and Electronics, Chinese Academy of Sciences, 610209 Chengdu, China

1 Introduction

The discovery potential of classical telescopes is mostly influenced by their optical diameter D , determining their ultimate angular resolution λ/D , and their collecting area, determining their light collection capability. These improve as D and D^2 respectively in conventional monolithic telescopes. These quantities are not independent unless the optical aperture is dilutely segmented as an array of N many smaller mirrors, the size d of which can be small compared to their spacing s . A very much higher resolution is then obtainable, without affecting the light collecting area D^2 , by spreading apart the small mirrors for a meta-aperture much larger than D , with a collecting area Nd^2 comparable to or exceeding D^2 .

Such systems are interferometers. They can grow for improved resolution by spreading apart the small mirrors, and for luminosity either by enlarging them or increasing their number. The second method is preferable, as discussed in Labeyrie 1996 [4], since it also improves the dynamic range of the images due to the better sampling of the optical wavefront.

The system becomes a hypertelescope, defined as a direct-imaging multi-element interferometer using a densified pupil, if a pupil densifier is added near the eyepiece or the focal camera. This is a small element which is an array of miniature Galilean beam-expanders, inverted for magnifying each sub-pupil within the meta-pupil. It means that the highly diluted entrance pupil is reimaged before the beam combination, to form the densified pupil as an homothetic map of the entrance pupil but where each subpupil has been magnified. As described in Labeyrie (1996) [4], Lardi re et al. 2007 [8], and Patru et al. 2007 [12], it intensifies the image as γ^2 , where γ is the subpupil magnification achieved by each beam-expander. Most light collected from a point source can then be concentrated into the interference peak, thus improving the overall light efficiency. This blaze effect occurs at the expense of sky coverage: the celestial field directly imaged at full resolution is then limited to a “Direct Imaging Field” (DIF) spanning $\lambda/(\gamma - 1)d$ ideally reaching the “Clean Field” (CF) spanning λ/s when $s = (\gamma - 1)d$, which corresponds to full densification, when the magnified sub-pupils become adjacent. It should be noted that this notion of “Clean Field” is not related to the hypertelescope principle, it is a general property of interferometers due to the sampling of the wavefront by the entrance pupil. The “Clean Field” matches the “dark zone” observable in the image of a point source, inside a wider and more intense annulus, containing speckles if the multi-aperture pattern is random or periodic peaks if it is periodic [8, 12]. However, separate imaging channels, spaced at least λ/d apart on the sky, and each covering the much smaller CF size, can be arranged for observing multiple sources such as a globular cluster, a remote galaxy, etc... The meta-aperture size of hypertelescopes may reach kilometers at terrestrial sites, owing to topographic and atmospheric limitations. But much larger meta-apertures, possibly reaching 100 km in diameter, appear feasible on the Moon and at space sites such as the Sun-Earth Lagrange point L2. The theory of hypertelescope imaging shows that pupil densification improves the efficiency of light concentration in the interference peak. Its energy content can become comparable to that provided by a conventional telescope having the same collecting area. Similarly high limiting magnitudes are then reachable, up to the $m_V = 36$ value of an adaptive ELT.

Most of the modern questions of Astrophysics can benefit from or even directly depend on an improved spatial resolution. This is particularly true in one of the ASTRONET priorities “What is the origin and evolution of stars and planets?”. This theme is usually structured around six main questions: How do stars form? Do we understand stellar structure and evolution? What is the life-cycle of the Interstellar Medium and Stars? How do planetary systems form and evolve? What is the diversity of planetary systems in the Galaxy? Is there evidence for Life on exoplanets? The recent results obtained on the VLTI [3] or on the CHARA Array [13] demonstrate the importance of optical long baseline interferometry and the unique constraints this technique can bring on all these questions.

To achieve these science goals, the future construction of an ambitious hypertelescope is considered. We also intend to bring an answer to the current situation of optical interferometry. The conceptual solutions that have been used for the last four decades are indeed probably not correctly adapted to an array of hundreds of apertures. The complexity of the Coudé trains, the multiplication of mirrors, and delay lines will probably prevent the construction of an equivalent of ALMA in the optical domain. However, the construction of an hypertelescope will have to face other challenges. We can summarize them as: 1/ identification of a correctly adapted site on ground or decision for space deployment, 2/ management of the motion of the focal optics and of the field of view, and 3/ cophasing for enhanced performance in precision and sensitivity. In this paper we present in Section 2 the prototype hypertelescope that we have started to build in the Southern Alps and we discuss the recent progress and the future activities in Section 3. In Section 4 we briefly describe other important activities that are engaged for preparing the solutions to the main questions presented above.

2 Presentation of the Ubaye hypertelescope project

The optimal pattern of sub-aperture arrangements for hypertelescopes depends on the type of source observed. The VLTI [2], the CHARA [13] and other telescope arrays having a beam-combiner for interferometry can be equipped with a pupil densifier for operating in the hypertelescope mode, as proposed for the Very Large Telescope [7]. The optical delay lines, generally needed by such arrays for compensating the effect of Earth rotation in the absence of a global steerable mount, implies a high cost when adding more telescopes, and thus restricts the number of apertures, thereby limiting the imaging performance. This performance can be much improved with the numerous apertures usable in the case of Arecibo-like architectures (also called Carlina), since they require no delay lines. They can therefore use hundreds of sub-apertures, thus allowing a far better imaging performance. The size limitation for steerable mounts is currently limiting the optical diameter of ELT's to about 40 m, instead of the kilometric size considered for terrestrial hypertelescopes [6]. With terrestrial Carlina architectures, the absence of a giant steerable mount for globally pointing the hypertelescope as a solid system causes an apparent drift of the sub-pupils pattern with respect to the metapupil seen from the focal receiver. This effect is not critical since the sub-pupil drift can be accommodated in the focal optics, and

it causes a form of aperture supersynthesis during long exposures which can improve the imaging performance.

To verify the level of tracking accuracy achievable in actual conditions with a suspended focal gondola, the team has installed and tested since 2011 some elements of the “Ubaye Hypertelescope” prototype in a high valley of the southern Alps [5], after the initial encouraging results of Le Coroller et al. 2015 [9]. Selected for its smooth curvature and East-West orientation, its topography favors near-meridian observing with a meta-aperture diameter potentially reaching 200m, and a larger metamirror size for annual coverage of the Northern celestial hemisphere. Unlike the massive suspended focal structure of the Arecibo radio-telescope, with its alt-azimuthal support for the large focal corrector and receiver, it has a much smaller focal package, with mass in the 20 kg range rather than hundreds of tons. A single suspension cable, 800 m long across the Moutière valley, carries the focal gondola 101 m above its floor (see Fig. 1). The cable, oriented North-South, can pendulate East-West to allow during an hour the diurnal tracking of a star by the gondola, which can also roll along it for declination adjustments. This is driven with millimeter accuracy by six thin cables, 1 mm² in section and made of high-modulus aramid fiber, attached to the gondola and actuated by small winches under computer control [1]. Their coordinated action drives the gondola’s all six degrees of freedom for adjusting its position and attitude. Servo-feedback is installed for automated tracking and focusing thanks to a camera installed in the gondola and with additional viewing systems on the primary segments (see Section 3).

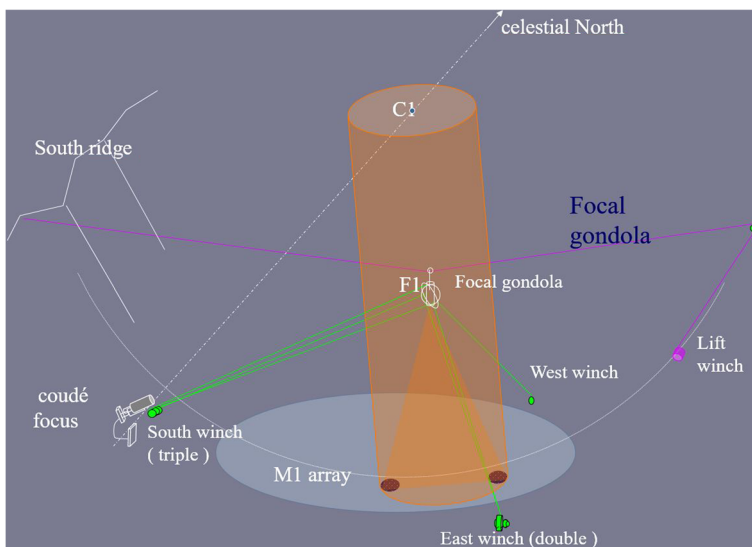


Fig. 1 Schematic representation of the driving system of the Ubaye hypertelescope prototype. The dilute primary mirror (light-blue) is fixed and co-focuses the drifting image of the observed source onto a movable focal camera. Suspended from a transverse cable (purple), it is driven by 6 oblique tethers (green), under computer control. The initial testing under way uses only two mirror segments (dark blue), 15 cm in diameter and spaced 15.8 m apart along the meridian. Hundreds are expected later within a meta-aperture expandable to 200 m

3 Recent progress and future activities

Four summers of construction and testing in the Moutière valley, at 2100–2300 m altitude, with a North-South pair of 20 cm M1 mirrors spaced 15.8 m apart, and a simplified version of the gondola optics for initial testing with two-aperture fringes, have demonstrated the validity of the scheme. In a two-aperture configuration, we can indeed replace the more general densifier [6] by a simplified arrangement of light-deviating wedge prisms, equivalent to Michelson's design at Mt Wilson, and similarly producing a densified pupil. The focal gondola is equipped with two cameras. The first one (MAKO) permits to obtain an image of the two stars and the two pupils for the alignment and tracking control. The second one (BASLER) is used for the science purpose and is fed by a low dispersion grism also equipped with an anamorphic optics for the correct adaptation of the spatial and spectral sampling. The optical setup of the gondola is presented in Fig. 2.

An electronic box controls the various systems installed on the gondola: wireless Internet and radio connection, laser diode, readout of the tension of the wires, control of the cameras, and radio transmission of their images. In the 2017-version of the optics simplified for the two-aperture case, we also used additional motorized optics permitting to finely tune the superposition of the two images with a tiltable plate and to change the optical path difference between the two upcoming beams with a pair of counter-moving optical wedges (see Fig. 3). These systems were finally not used because of the redundancy with the possible tip/tilt and piston on the primary segments themselves. The required power is distributed by LiPo batteries that can go up and down from the ground thanks to a manual elevator and three electric contacts.

The automatic control software successfully achieved the gondola tracking with the specified millimetric accuracy required to stabilize the direct interferometric image on the sensitive area of the detector. In 2017 we have been able to achieve this performance during more than 40 min after the initial alignment. In the current configuration of the installation, the tracking is limited to ± 30 mn around the meridian transit by the balance of tensions on the driving wires. Real-time control of these tensions is performed and the readout of the values is remotely possible. The images of the cameras are remotely transmitted to the ground station to allow a real-time control of the images. Preliminary tests of a full autoguiding, with the cameras installed on the gondola have been performed but, for the moment, occasional fine corrections have to be typed on the computer's keyboard. They permit to correct the East-West, North-South positions of the gondola as well as their heights above the array. They also control the triaxial orientation of the focal optics.

Although we were successful in 2015 in obtaining an image of the star Vega on the gondola, this step was not achieved in 2017 because of a shorter campaign and also of difficulties related to the first tests on sky of the new viewer system presented in Fig. 4.

The guider's camera or eyepiece sees the star image (in blue) through the hologram, with zero-order diffraction, and also the first-order diffracted image (in green) of a point source, in the form of a laser diode beacon located at the focal gondola's entrance. Its downgoing diverging light is collimated by the M1 mirror toward the star, when the mirror is correctly oriented. Part of the upgoing collimated laser light

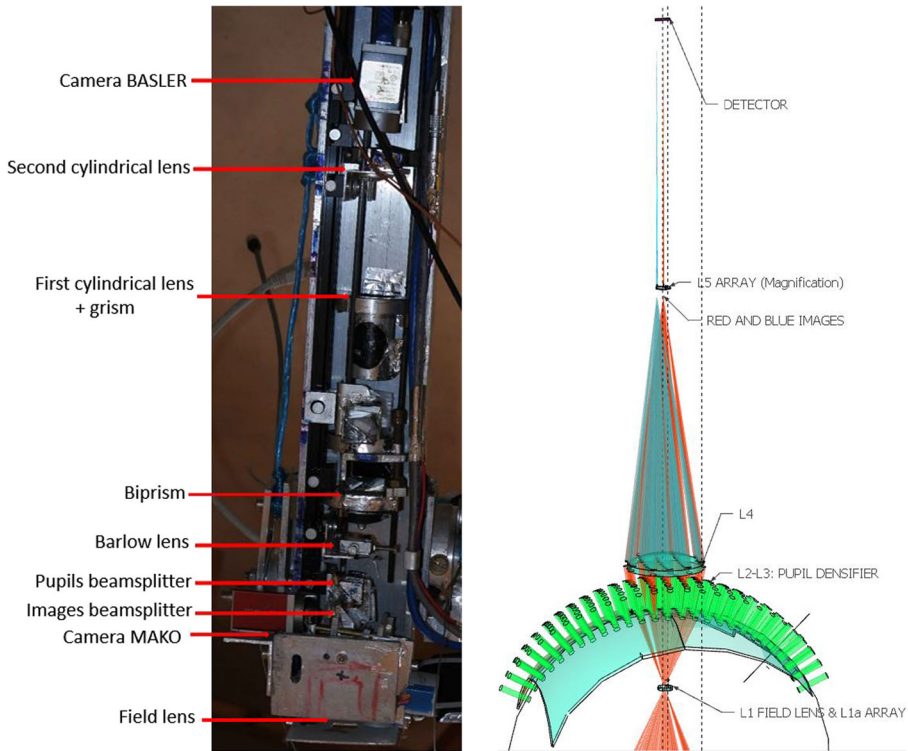


Fig. 2 Beam combining optics in the focal gondola. At left the simplified testing version restricted for two beams. It is a miniature equivalent of Michelson’s beam combiners at Mt Wilson, here using two pairs of wedge prisms instead of mirrors. Two motors control the optical path difference and the image superposition (see details in Fig. 3). At right, the full version, under development for many beams. It contains a small equatorial mount which directs the main optical train toward the observed stars’s sky position, while the pupil densifier dome (green) is rigidly attached to its virtual pier for keeping a fixed attitude, as needed for accommodating the pupil’s apparent drift while the gondola tracks the star’s Fizeau focal image. Beams from a red star are co-focused by the primary mirror segments, arrayed as a paraboloidal meta-mirror, located far below, as a Fizeau image on a field lens L1, which re-images each sub-pupil at the entrance of the corresponding beam-densifier element (lenses L2 and L3 in each green tube). The image is combined by lens L4 and further magnified by lens L5 on the science camera, through an optional grism disperser (not shown). Light from a blue star is similarly processed, although in a separate optical channel separated by a microlens array L1a laminated onto L1, and the L2 lenses in each densifier element are also arrays projecting sub-pupils which are superposed onto the following L3 lens. L5 is also in fact an array of magnifier lenses, providing adequate sampling

is focused by diffraction through the hologram onto the small “cat’s retina” mirror, which reflects it back through the hologram, where it becomes re-collimated by first-order diffraction and co-propagating with the star’s light, thanks to the specific properties of the hologram plate. The vector spacing of both spots on the camera is the error signal to be corrected for maintaining the star’s image at the gondola’s entrance. The correction is achievable either by tip-tilting the M1 mirror or by moving the gondola. If the M1 co-spherization has been previously adjusted, for example with similar guiders attached to each M1 mirror, the latter method is obviously preferable

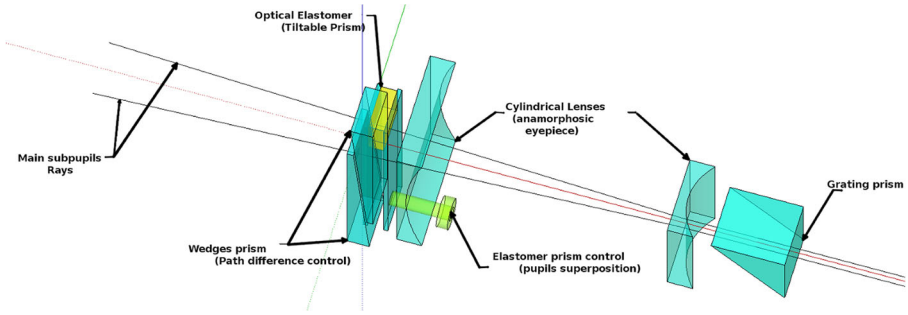


Fig. 3 Optical principle of the science beam in the 2-mirror simplified configuration. One of the beam goes through a tilttable prism allowing a fine tuning of the superposition of the two images. The optical path difference could be adjusted by translatable wedge prisms. An anamorphic optic and a grism constitute the main optics of the dispersion system adapted to the correct sampling of dispersed fringes

for preserving the co-spherization, and it is usable for auto-guiding the gondola. The hologram, patterned as a Fresnel zone, is fabricated with the recording arrangement shown at right, using the same laser, and which ensures zero spherical aberration. Together with the retina mirror, it is supposed to behave as a compact cat’s eye reflector. This is in this last property that we have had difficulties during our last campaign. We have indeed identified an error of a few millimeters in the focus of the retina mirror, while the required precision should be of the order of $100 \mu\text{m}$. That has generated an unknown difference between the correct superposition in the eyepiece and

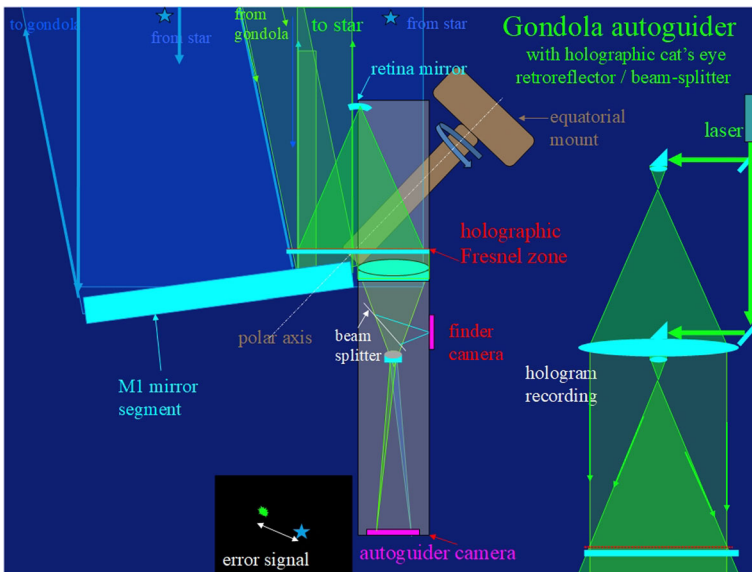


Fig. 4 Left: schematic drawing of cat’s eye retro-reflector used for aligning the focal gondola with the star’s image. The superposition error of the star (blue) and gondola beacon (green) spots on the camera is the error signal fed to the gondola’s guiding system. Right: representation of the laser recording scheme for fabricating the hologram with a flat and diverging wave

the actual superposition at the entrance of the gondola. This will be corrected in the future thanks to more in-depth testing in laboratory.

4 Other complementary studies toward the development of an ambitious hypertelescope

In parallel to the activities presented above, our team is also progressing on the study of the different aspects, critical for the implementation of an ambitious hypertelescope. The first one is related to the main science cases that a hypertelescope could address and is thus related to the field of view limitation. As a sub-product of this study, we also consider the possibility, as it is done on the FAST radio telescope [10], to go from a spherical shape to a deformable parabolic shape for the primary diluted mirror. And finally we shortly present the studies made to adapt the principle of a laser guide star for hypertelescope in order to reach much fainter magnitude in the future.

4.1 Overcoming the field of view limitation

The spherical shape of the primary diluted mirror in the Carlina/Ubaye design requires a corrector of spherical aberration, currently implemented in the form of a Mertz corrector. But the primary meta-mirror can be adaptively parabolized, like in the FAST radio telescope [10], for an aberration-free image in the axis. Clustered compact sources can however be simultaneously imaged at high resolution by arranging an array of imaging channels, dissected by a matching array of field-lenses in the Fizeau focal plane. The field aberrations appearing within the off-axis channels, mostly coma, are correctible separately in each of them, as discussed by Xie et al. (in preparation), if the M1 meta-mirror is actively parabolized. An array of aspheric L5 lenses suffices for separate coma correction in each sub-field: no need for separate actuator arrays in each, except if the total field is larger than the atmospheric isoplanatic patch. The troublesome coma in the off-axis sub-fields caused by the primary mirror could indeed be considered in each small subfield as tilt and piston. Thanks to a Zemax simulation using tip/tilt-piston actuators for optimized co-phasing, we verified successfully that the theoretical direct image of a point source is obtained with the expected λ/D resolution of the meta-aperture.

4.2 Active primary segments for a deformable parabolic primary diluted mirror

As seen before, a large fraction of the aberration generated by the fixed spherical mirror could easily be reduced if one considers an adaptive parabolization. With the Ubaye configuration, a simple solution is to motorize each primary segment with three sub-micrometers actuators to allow slow tip/tilt and piston correction to position the segment on the instantaneous parabola. With 15 cm segments for a 200 m diameter of the meta-mirror, it can be shown that the required deformation of the small spherical segment is totally negligible. The difference between the sphere and the parabola could easily be established as $\Delta(x) = \frac{x^4}{8R^3}$, with R the radius of curvature and x the off-axis position of the considered segment. For a meta-mirror with a radius

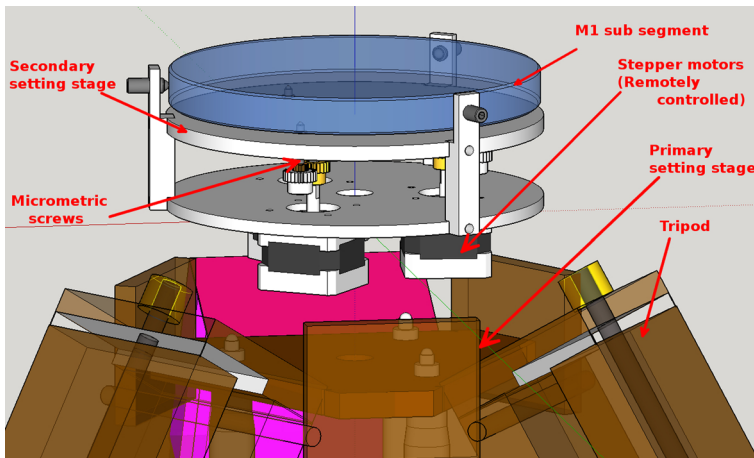


Fig. 5 Mechanical design of the new motorized tripod for an active paraboloidal meta mirror. The shallow concave mirror segments (blue) can remain spherical while matching the paraboloid within Rayleigh's tolerance. Only three motorized screws are needed for adjusting the tip, tilt, and piston

of curvature $R = 200$ m, a variation of pointing of $\pm 15^\circ$ generates a difference of piston of ± 100 mm.

As presented in Fig. 5, we have started the design and integration of motorized actuators on the main tripods and expect to test them in the coming months.

4.3 Laser guide star for hypertelescope

Nunez et al. [11] have investigated the feasibility of using a modified laser-guide-star technique that is suitable for large diluted apertures. The method consists of using subsets of apertures to form fringes in the sodium layer as a possible way to perform wavefront sensing with diluted apertures. This solves the problem of resolving the artificial star since the same subset of apertures is used to form the artificial star/fringes and to perform wavefront sensing by re-imaging the fringes, which contain optical path difference information. The use of several laser guide stars can in principle solve the classical cone effect problem due to the finite distance of the artificial star. Preliminary tests in the laboratory have permitted to validate the technique in the case of a single laser guide star, and with signal to noise ratios comparable to those predicted by simulations. Aside from all the engineering feats that must be undertaken, the current main limitation of this technique is that the proposed phase-unwrapping method requires too many photons, and thus very powerful lasers.

5 Conclusion

In this paper we have given an overview of the most recent activities done in our team for the progress of the hypertelescope principle. The feasibility of a fixed

diluted primary with a movable focal optics has been verified with a computer-driven gondola suspended from a 800 m cable. The main limitations of the current interferometers in terms of field of view and sensitivity are also discussed.

Acknowledgments We wish to warmly thank all the volunteers that have spent part of their time in helping for the development and the test of the Ubye hypertelescope in 2017: Jean-Paul Amerigo, Christian Caly, Patrick Comminges, Roger Croix, Alain Grimaud, Bruno Lacamp, Jerome Maillot, Gerald Mauboussin, Monique Meyran, Cedric et Stephanie Monasse, Jordi Pijoan, Remi Prudhomme, Martine Roussel, Eric Salgon, Patrick Sem, Arun Surya, and Florian Taillandier. These progresses will not have been possible without their contributions. We also thank Isabelle Tallon-Bosc for her critical reading of an earlier version of the paper.

References

1. Enmark, A., Andersen, T., Owner-Petersen, M., Chakraborty, R., Labeyrie, A.: Integrated model of the Carlina Telescope. In: Integrated modeling of complex optomechanical systems, vol. 8336, p. 83360J (2011). <https://doi.org/10.1117/12.921015>
2. Glindemann, A., Albertsen, M., Andolfato, L., Avila, G., Ballester, P., Bauvir, B., Delplancke, F., Derie, F., Dimmler, M., Duhoux, P., di Folco, E., Frahm, R., Galliano, E., Gilli, B., Giordano, P.N., Gitton, P.B., Guisard, S., Housen, N., Hummel, C.A., Huxley, A., Karban, R., Kervella, P., Kiekebusch, M., Koehler, B., Leveque, S.A., Licha, T., Longinotti, A., McKay, D.J., Menardi, S., Monnet, G.J., Morel, S., Paresce, F., Percheron, I., Petr-Gotzens, M., Phan Duc, T., Pott, J.U., Puech, F., Rantakyro, F.T., Richichi, A., Sabet, C., Scales, K.L., Schoeller, M., Schuhler, N., van den Ancker, M., Vannier, M., Wallander, A., Wittkowski, M., Wilhelm, R.C.: VLTI technical advances: present and future. In: Traub, W.A. (ed.) Society of Photo-Optical Instrumentation Engineers (SPIE) Conference Series, Presented at the Society of Photo-Optical Instrumentation Engineers (SPIE) Conference, vol. 5491, pp. 447–+ (2004)
3. GRAVITY Collaboration, Abuter, R., Accardo, M., Amorim, A., Anugu, N., Ávila, G., Azouaoui, N., Benisty, M., Berger, J.P., Blind, N., Bonnet, H., Bourget, P., Brandner, W., Brast, R., Buron, A., Burtscher, L., Cassaing, F., Chapron, F., Choquet, É., Clénet, Y., Collin, C., Coudé du Foresto, V., de Wit, W., de Zeeuw, P.T., Deen, C., Delplancke-Ströbele, F., Dembet, R., Derie, F., Dexter, J., Duvert, G., Ebert, M., Eckart, A., Eisenhauer, F., Esselborn, M., Fédou, P., Finger, G., Garcia, P., Garcia Dabo, C.E., Garcia Lopez, R., Gendron, E., Genzel, R., Gillessen, S., Gonte, F., Gordo, P., Grould, M., Grözinger, U., Guieu, S., Haguenaer, P., Hans, O., Haubois, X., Haug, M., Haussmann, F., Henning, T., Hippler, S., Horrobin, M., Huber, A., Hubert, Z., Hubin, N., Hummel, C.A., Jakob, G., Janssen, A., Jochum, L., Jocou, L., Kaufer, A., Kellner, S., Kern, L., Kervella, P., Kiekebusch, M., Klein, R., Kok, Y., Kolb, J., Kulas, M., Lacour, S., Lapeyrère, V., Lazareff, B., Le Bouquin, J.B., Lèna, P., Lenzen, R., Lévêque, S., Lippa, M., Magnard, Y., Mehrgan, L., Mellein, M., Mérand, A., Moreno-Ventas, J., Moulin, T., Müller, E., Müller, F., Neumann, U., Oberti, S., Ott, T., Pallanca, L., Panduro, J., Pasquini, L., Paumard, T., Percheron, I., Perraut, K., Perrin, G., Pflüger, A., Pfuhl, O., Phan Duc, T., Plewa, P.M., Popovic, D., Rabien, S., Ramírez, A., Ramos, J., Rau, C., Riquelme, M., Rohloff, R.R., Rousset, G., Sanchez-Bermudez, J., Scheithauer, S., Schöller, M., Schuhler, N., Spyromilio, J., Straubmeier, C., Sturm, E., Suarez, M., Tristram, K.R.W., Ventura, N., Vincent, F., Waisberg, I., Wank, I., Weber, J., Wieprecht, E., Wiest, M., Wierzorrek, E., Wittkowski, M., Woillez, J., Wolff, B., Yazici, S., Ziegler, D., Zins, G.: First light for GRAVITY: phase referencing optical interferometry for the very large telescope interferometer. ArXiv e-prints (2017)
4. Labeyrie, A.: Resolved imaging of extra-solar planets with future 10–100 km optical interferometric arrays. *Astron. Astrophys. Suppl. Ser.* **118**, 517–524 (1996)
5. Labeyrie, A., Allouche, F., Mourard, D., Bolgar, F., Chakraborty, R., Maillot, J., Palitzyn, N., Poletti, J.R., Rochaix, J.P., Prud'homme, R., Rondi, A., Roussel, M., Surya, A.: Construction of a 57 m hypertelescope in the Southern Alps. In: *Optical and Infrared Interferometry III*, vol. 8445, p. 844511 (2012). <https://doi.org/10.1117/12.926168>
6. Labeyrie, A., Mourard, D., Allouche, F., Chakraborty, R., Dejonghe, J., Surya, A., Bresson, Y., Aime, C., Mary, D., Carlotti, A.: Concept study of an Extremely Large Hyper Telescope (ELHyT) with

- 1200 m sparse aperture for direct imaging at 100 micro-arcsecond resolution. In: *Optical and Infrared Interferometry III*, vol. 8445, p. 844512 (2012). <https://doi.org/10.1117/12.926541>
7. Lardiere, O., Labeyrie, A., Mourard, D., Riaud, P., Arnold, L., Dejonghe, J., Gillet, S.: VIDA (Vlti Imaging with a Densified Array), a densified pupil combiner proposed for snapshot imaging with the VLTI. In: Traub, W.A. (ed.) *Interferometry for Optical Astronomy II*, vol. 4838, pp. 1018–1027 (2003). <https://doi.org/10.1117/12.459076>
 8. Lardièrè, O., Martinache, F., Patru, F.: Direct imaging with highly diluted apertures—I. Field-of-view limitations. *MNRAS* **375**, 977–988 (2007). <https://doi.org/10.1111/j.1365-2966.2006.11362.x>
 9. Le Coroller, H., Dejonghe, J., Hespels, F., Arnold, L., Andersen, T., Deram, P., Ricci, D., Berio, P., Blazit, A., Clause, J.M., Guillaume, C., Meunier, J.P., Regal, X., Sottile, R.: The Carlina-type diluted telescope. Stellar fringes on Deneb. *Astron. Astrophys.* **573**, A117 (2015). <https://doi.org/10.1051/0004-6361/201424623>
 10. Nan, R.: Introduction to FAST: five hundred meter aperture spherical radio telescope. In: *Ground-based and Airborne Telescopes II*, vol. 7012, p. 70121E (2008). <https://doi.org/10.1117/12.791288>
 11. Nuñez, P.D., Labeyrie, A., Riaud, P.: Towards laser guide stars for multi-aperture interferometry: an application to the hypertelescope. *MNRAS* **439**, 1787–1795 (2014). <https://doi.org/10.1093/mnras/stu061>
 12. Patru, F., Mourard, D., Lardièrè, O., Lagarde, S.: Optimization of the direct imaging properties of an optical-fibred long baseline interferometer. *MNRAS* **376**, 1047–1053 (2007). <https://doi.org/10.1111/j.1365-2966.2006.11317.x>
 13. ten Brummelaar, T.A., McAlister, H.A., Ridgway, S.T., Bagnuolo W.G. Jr., Turner, N.H., Sturmman, L., Sturmman, J., Berger, D.H., Ogden, C.E., Cadman, R., Hartkopf, W.I., Hopper, C.H., Shure, M.A.: First results from the CHARA Array. II. A description of the instrument. *ApJ* **628**, 453–465 (2005). <https://doi.org/10.1086/430729>